

Quantum liquid crystals of helium monolayers

S. Nakamura^a, K. Matsui^b, T. Matsui^b, and Hiroshi Fukuyama^{a,b*}

^a*Cryogenic Research Center, The University of Tokyo,
2-11-16 Yayoi, Bunkyo-ku, Tokyo 113-0032, Japan and*

^b*Department of Physics, The University of Tokyo,
7-3-1 Hongo, Bunkyo-ku, Tokyo 113-0033, Japan*

(Dated: February 8, 2016)

The second-layer phase diagrams of ^4He and ^3He adsorbed on graphite are investigated. Intrinsically rounded specific-heat anomalies are observed at 1.4 K and 0.9 K, respectively, over extended density regions in between the liquid and incommensurate solid phases. They are identified to anomalies associated with Kosterlitz-Thouless-Halperin-Nelson-Young type two-dimensional melting. The prospected low temperature phase (C2 phase) is either a commensurate quantum solid containing *zero-point defectons* or a *quantum hexatic* phase with quasi bond-orientational order. In any case, this would be the first atomic realization of *quantum liquid crystal*, a new state of matter. From the large enhancement of the melting temperature over ^3He , we propose to assign the observed anomaly of ^4He -C2 phase at 1.4 K to the hypothetical supersolid or superhexatic transition.

PACS numbers: 67.80.dm, 67.10.Hk, 67.80.bd, 64.70.mj

Quantum liquid crystal (QLC) is a novel state of matter in nature. It is quantum liquid with partially broken rotational and/or translational symmetries and, from another perspective, it is solid with fluidity (or superfluidity) even at $T = 0$. The electronic nematic phase, which is conceptually one of the QLCs, is recently being studied in a variety of materials [1, 2]. Atomic or molecular QLCs are more intuitive and direct quantum counterparts of classical liquid crystal. In the case of bosonic systems, one of the hallmarks of QLC is supersolidity. Recently the search for supersolidity has intensively been made in bulk solid ^4He [3–5] and is proposed in cold atoms or molecules trapped in optical lattices [6]. The predicted stripe phase of superfluid ^3He in slab geometry is a candidate for fermionic QLC [7, 8]. However, all previous experimental attempts to detect atomic or molecular QLCs have not yet been successful or still are under debate.

Atomic monolayer of helium (He) adsorbed on a strongly attractive graphite surface provides a unique arena to investigate novel quantum phenomena of bosons (^4He : spinless) and fermions (^3He : nuclear spin 1/2) in two dimensions (2D). Particularly the prospected commensurate phase in the second layer of He (hereafter the C2 phase) is a hopeful candidate for atomic QLC because of a delicate balance among the kinetic, He-He interaction and corrugated potential energies. The commensurability here is with respect to the triangular lattice of the compressed first He layer. The gapless quantum spin-liquid state [9] and the anomalous thermodynamic behaviour in the ^3He -C2 phase [10] can be signatures of the inherent fermionic QLC nature [11].

If the ^4He -C2 phase is a QLC, the supersolid ground state can be expected. Eventually, two previous torsional oscillator experiments on this system observed a reentrant superfluid response as a function of density below 0.4 K [12, 13]. However, the identification of the phenomenon is left controversial, since the detected super-

fluid fractions are limited to 0.01–0.02, and the density regions where the superfluid responses are detected are not quantitatively consistent with each other. These are presumably due to the poor connectivity of microcrystallites (platelets) and the existence of heterogeneous surfaces (about 10% of the total [14]), which results in ambiguity of density scale, in Grafoil substrate they used.

So far, the ^4He -C2 phase has been believed to exist from the large specific-heat anomaly observed at $T \approx 1.5$ K [15] in a narrow density range between the liquid (L2) and incommensurate solid (IC2) phases. Though a similar anomaly has been found in ^3He , too, at $T \approx 0.9$ K at one density [16], other details are not known. Instead, the existence of the ^3He -C2 phase has been accepted from the various nuclear magnetic properties at low mK [9].

The previous belief on the ^4He -C2 phase has recently been thrown into doubt by the path integral Monte Carlo (PIMC) calculation by Corboz *et al.* [17]. Unlike the previous PIMC calculations [18], they claimed the instability of the C2 phase against the L2 and IC2 phases, if zero-point vibrations of the first layer atoms are explicitly taken into account. Their claim raised serious questions: Are the specific-heat peaks observed in ^4He and ^3He the same phenomenon related to 2D melting? Isn't the observed C2 phase stabilized artificially by finite size effects due to the platelet structure of exfoliated graphite substrate?

In this Letter, we report results of new high-precision heat-capacity measurements of the second layers of pure ^4He and ^3He films at temperatures from 0.1 to 1.9 K using a ZYX exfoliated graphite substrate. ZYX is known to have ten times larger platelet size (100–300 nm) [19] than Grafoil, a substrate used in all previous works. An average number of He atoms adsorbed on an atomically flat platelet in ZYX is 10^6 which is more than 10^3 times larger than that in the simulation of Ref. 17. We obtained unambiguous thermodynamic evidences for the

existence of a distinct phase (C2 phase) between the L2 and IC2 phases regardless of system size and for that the phase exists over an extended density range in both isotopes. The results strongly support the QLC hypothesis for the C2 phase. From the observed anomalous isotope effects on melting temperature and entropy release, we propose a supersolid or superhexatic phase transition of Kosterlitz-Thouless-Halperin-Nelson-Young (KTHNY) type [20] based on binding/unbinding of topological defects in the ^4He -C2 phase at a temperature below 1.4 K.

The experimental setup used here has been described in detail elsewhere [21]. The heat capacity was measured by the heat pulse method with variable constant heat flows. In the following we show only the heat capacity of adsorbed He films after subtracting the addendum (empty cell) and the desorption contribution (see below). The surface area of the ZYX substrate is $30.5 \pm 0.2 \text{ m}^2$. The vapor pressure of sample is monitored with an *in situ* capacitive strain gauge.

The much larger platelet size of ZYX than Grafoil is well demonstrated by a two times higher specific heat peak at the order-disorder transition ($T = 2.9 \text{ K}$) for the $\sqrt{3} \times \sqrt{3}$ commensurate phase (C1 phase) of ^4He adsorbed directly on graphite (see Fig. 1 of Ref. 22) and for that of ^3He as well [23]. The commensurability of the C1 phase is with respect to the graphite honeycomb lattice. The critical T -region is also wider in ZYX being consistent with the finite size scaling. Despite the larger platelet size, ten times smaller specific surface area ($2 \text{ m}^2/\text{g}$) of ZYX causes much larger desorption heat-capacity contribution. This prevents us from analyzing present experimental data with reasonable accuracies at temperatures higher than 1.8–1.9 and 1.3–1.4 K for ^4He and ^3He , respectively.

Let us first show T -dependencies of measured heat capacities (C) of ^4He films. The data taken at densities of $17.50 \leq \rho \leq 19.73 \text{ nm}^{-2}$ are shown in Fig. 1(a), and those at $19.73 \leq \rho \leq 21.01 \text{ nm}^{-2}$ in Fig. 1(b). Here ρ is the total areal density. Since the first-layer has a much higher density or Debye temperature than the second layer, the contribution to C is less than 3% in the T -range we studied. At the lowest ρ (17.50 nm^{-2}) the system is a uniform 2D liquid. At high T , this phase is characterized by a nearly constant C slightly less than the $N_2 k_B$ value expected for an ideal 2D gas as well as a broad maximum near 0.9 K below which C rapidly falls down [15, 23]. Here N_2 is the number of He atoms in the second layer which is calculated from the known first-layer density (ρ_1) vs. ρ relation obtained from the neutron scattering data [24] using the second-layer promotion density of $11.8 \pm 0.3 \text{ nm}^{-2}$ [22]. For example, $\rho_1 = 12.05 \pm 0.3 \text{ nm}^{-2}$ at $\rho = 19.73 \text{ nm}^{-2}$.

As ρ increases above 18.70 nm^{-2} , a new C anomaly starts to develop near $T = 1.4 \text{ K}$ whereas the liquid component gradually decreases. The two features coexist un-

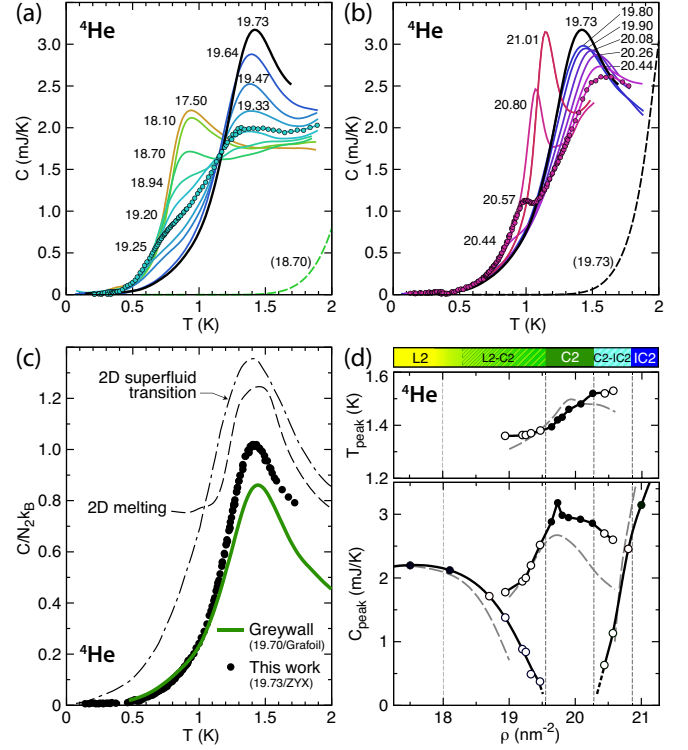


FIG. 1. (a) (b) Heat capacities of the second layer of ^4He on ZYX graphite. The numbers are total densities in nm^{-2} . For clarity actual data points are plotted only for 19.25 and 20.57 nm^{-2} . The dashed lines are desorption contributions which have already been subtracted from the raw data. (c) Specific heat of the C2 phase obtained with ZYX (filled circles: this work) and Grafoil (solid line: Ref. 15) substrates. Also shown are calculated specific heats for 2D melting (dashed line: Ref. 25) and superfluid transition (dash-dotted line: Ref. 26), in which the T -scales are normalized by T_{peak} . (d) Density variations of C_{peak} (lower panel) and T_{peak} (upper panel). The filled symbols are for the pure L2, C2 and IC2 phases and open ones for the coexistence regions. The dashed lines are the data of Ref. 15 adjusted to our surface area.

til 19.47 nm^{-2} . Above 19.64 nm^{-2} the liquid component completely disappears leaving only the rounded peak at 1.4 K which corresponds to the C2 peak observed by Greywall [15] using Grafoil substrate. As we further increase ρ , the heat-capacity peak height (C_{peak}) becomes largest at 19.73 nm^{-2} ($\equiv \rho_{C2}$) and then turns to decrease. In Fig. 1(c) the specific heat data at $\rho = \rho_{C2}$ obtained with ZYX and Grafoil are compared. They look similar each other except that the ZYX data give a slightly larger specific heat around the peak temperature T_{peak} by about 13%. Above 20.44 nm^{-2} a new peak appears near 0.8 K. With increasing ρ , the peak grows rapidly in height and temperature up to 1.2 K coexisting with the C2 anomaly which diminishes gradually keeping T_{peak} fixed. The two features apparently coexist at least until 20.80 nm^{-2} . This last peak is associated with melting transition of the IC2 solid [15, 23].

In Fig. 1(d) we plot density variations of C_{peak} and T_{peak} as well as those of Greywall [15] (dashed lines) who used Grafoil substrate. The phase diagram determined in this work is also shown on the top. Unambiguously, there exists a distinct C2 phase over an extended density region from 19.6 to 20.3 nm^{-2} where we observed only the C2 anomaly (closed circles). The C2 phase is definitely not an experimental artifact caused by finite size effects of substrate since the specific heat anomaly is even enhanced slightly with increasing the platelet size by an order of magnitude. Within this C2 region, T_{peak} increases by 10%. The C2 phase is well separated from the L2 and IC2 phases by L2-C2 ($18 < \rho < 19.6 \text{ nm}^{-2}$) and C2-IC2 ($20.3 < \rho < 20.9 \text{ nm}^{-2}$) coexistence regions where we observed the double anomaly feature (open circles). Although the feature is vaguely visible in Greywall's data at 19.00 and 20.30 nm^{-2} (see Fig. 3 of Ref. 15), it is much clearer with great details here thanks to finer ρ - and T -grids and the better substrate quality. For example, when ρ approaches ρ_{C2} from both directions, the L2 and IC2 anomalies destruct preferentially from higher- T envelopes keeping common low- T envelopes, while the C2 anomaly grows without changing its T_{peak} so much. This unusual behaviour can never be expected from the conventional phase separation (see the latter discussions).

Next we show heat capacity data of the second layer of ^3He films at densities of $17.50 \leq \rho \leq 19.00 \text{ nm}^{-2}$ in Fig. 2(a) and $19.00 \leq \rho \leq 20.40 \text{ nm}^{-2}$ in Fig. 2(b). The density evolution is qualitatively similar to that in ^4He . We observed again a clear C2 peak which becomes maximum at $\rho_{\text{C2}} = 19.1 \pm 0.1 \text{ nm}^{-2}$ and $T_{\text{peak}} = 1.0\text{--}1.1 \text{ K}$. This specific heat peak is very similar to that observed by Van Sciver and Vilches using Grafoil substrate [16] as compared in Fig. 2(c), indicating almost no size effects. Here we estimated N_2 assuming $\rho_1 = 11.6 \text{ nm}^{-2}$. The ρ_1 value is evaluated from the second-layer promotion density ($= 11.2 \pm 0.2 \text{ nm}^{-2}$) [23] and the subsequent first-layer compression by 4% [24].

In Fig. 2(d) we plot density variations of C_{peak} and T_{peak} for ^3He as well as a proposed phase diagram at $T = 0$. The determination of each phase boundary is somewhat ambiguous compared to ^4He , because the density grid of measurement is not fine enough here. The double anomaly feature in the coexistence regions is hardly visible due to weakly T -dependent large C contributions from Fermi liquids in the second and third layers. These contributions are represented by the heat capacity isotherm at $T = 0.2 \text{ K}$ plotted in Fig. 2(d). Note that the third layer promotion in ^3He occurs at a relatively low density ($\approx 19.3 \text{ nm}^{-2}$) before the C2-IC2 coexistence starts [23, 27]. This is in sharp contrast to the case of ^4He where the third layer promotion occurs at much higher densities ($\rho \geq 21 \text{ nm}^{-2}$) after the C2-IC2 coexistence completes [15]. The previous workers' data with Grafoil are consistent with our phase diagram if their density scales are multiplied by 1.015 for Refs. 16, 28 and 1.04

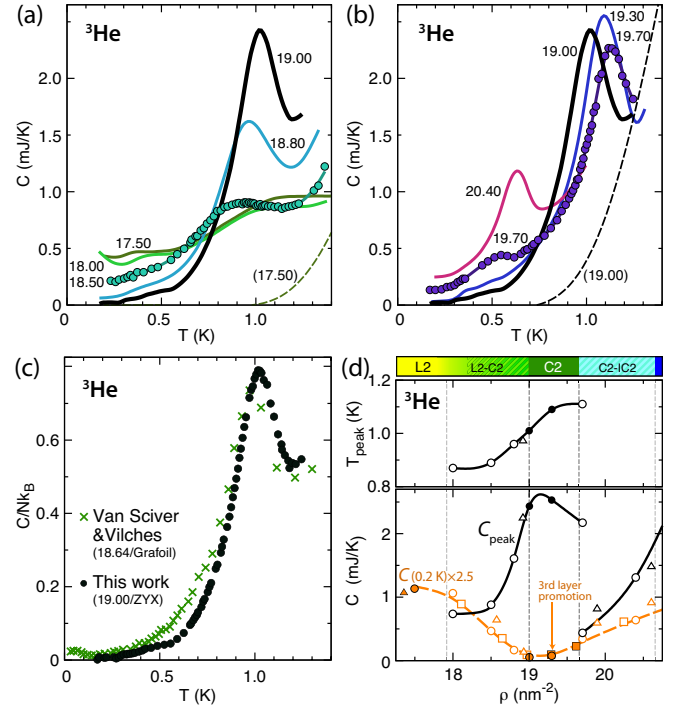


FIG. 2. (a) (b) Heat capacities of the second layer of ^3He on ZYX. (c) Specific heat of the C2 phase obtained with ZYX (filled circles: this work) and Grafoil (crosses: Ref. 16). The latter show slightly larger specific heats at low- T due to a small amount of remnant L2 phase. (d) Density variations of C_{peak} (lower panel) and T_{peak} (upper panel). The dashed line is a heat capacity isotherm at $T = 0.2 \text{ K}$. The triangles (Refs. 16, 28) and squares (Ref. 27) are the data with Grafoil adjusted to our surface area and density scale (see text). Other details are the same as Fig. 1.

for Ref. 27, 28.

There are many reasons to believe that the broad specific-heat anomalies observed in ^4He and ^3He are due to *continuous* 2D melting transitions of the C2 phase which possesses some type of spatial order. First, entropy changes associated with them, $\Delta S = 0.4\text{--}0.5 N_2 k_B$, are large enough to convince the presence of phase transitions (see Fig. 3(a)). Second, the anomalies look qualitatively similar between the two isotopes though they obey different quantum statistics. Third, the anomalies are substantially broad and the broadness is insensitive to the system size. Eventually, they are similar to the Monte Carlo simulation for melting of a 2D classical Lennard-Jones solid [25], which is consistent with the KTHNY theory, as shown in Fig. 1(c). In the same figure we also plot the specific-heat anomaly for the superfluid transition of 2D liquid ^4He [26] as a typical example of the Kosterlitz-Thouless type transition. Generally, the KTHNY theory predicts 2D solid to melt through two continuous transitions on warming, i.e., a transition from solid to hexatic and that from hexatic to uniform liquid. Both are accompanied by intrinsically rounded specific-

heat anomalies due to proliferation of free dislocations and disclinations, respectively. The peaks will be centered at 10–30% higher temperatures than the true transition temperatures at which practically no anomalies are observed [25].

Let us discuss the nature of the C2 phase in more detail. If it is a commensurate solid stabilized by a periodic potential from the first layer as was originally anticipated [29], we should assume the existence of sizable amount of zero-point defectons (ZPDs) [30] such as vacancies, interstitials, dislocations, domain walls, etc., which move quantum mechanically in a fixed triangular lattice. Otherwise, it is difficult to explain why the commensurate phase can be stabilized over a relatively wide density region of $w \equiv \Delta\rho_{C2}/\rho_{C2} \approx 0.08\text{--}0.09$ where we observed only the C2 anomaly and the growth of T_{peak} with increasing ρ . The neutron scattering data [24] with ZYX substrate show a small but steep increase by 1.3–1.5% of ρ_1 at densities near the L2-C2 coexistence and the C2 regions. This suggests a simultaneous compression of the first and second layers supporting the commensurate solid picture. It should, however, be noted that the neutron experiments were unsuccessful to detect Bragg peaks directly from the C2 phase. Also, we did not observe the two-stage transition. The former may be indicative of very large Debye Waller factor due to the weak oscillation amplitude of the periodic potential (~ 0.5 K [23]) and strong quantum fluctuations. The latter does not necessarily exclude the two-step transition because the two successive peaks can easily merge into a broader single peak if the transition temperatures are close enough.

Perhaps, a more plausible picture of the C2 phase is the quantum liquid with the short-range hexatic correlation, the *quantum hexatic* phase. The hexatic phase was first proposed as an intermediate phase in the two-stage

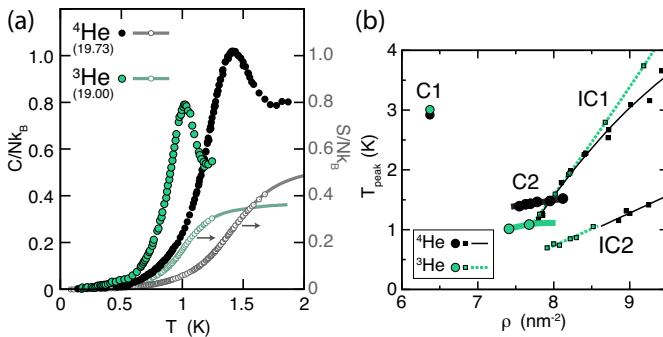


FIG. 3. (a) Specific-heat anomalies and entropy changes deduced from them for the ^4He - and ^3He -C2 phases. The lines for the entropies are extrapolations assuming mirror symmetry of $C(T)$ about $T = T_{\text{peak}}$. (b) Specific-heat peak temperatures T_{peak} of melting anomalies of various 2D He solids on graphite (Refs. 15, 23, 28, 31, 32). The C2 phase shows an anomalously inverted isotope effect (see text). IC1 is the incommensurate solid phase in the first layer.

melting of 2D solids [33]. It possesses only the quasi long-range order of the sixfold bond-orientational correlation, which spatially decays with a power law, not the translational order. This picture can explain the experimental and theoretical constraints more reasonably, e.g., the lack of translational long-range order in the neutron experiments [24] and the latest PIMC calculation [17], and rather close areal densities ($\rho_{C2} = 7.5\text{--}7.7 \text{ nm}^{-2}$) between ^3He and ^4He in spite of their different ρ_1 values [34]. In addition, within this model, the common low- T envelopes observed in the L2-C2 and C2-IC2 coexistence regions of ^4He can be interpreted by that the short-range C2 (or hexatic) correlation does not affect the excitation spectrum at low momenta as the *roton*-like softening near solidification computed for 2D liquid ^4He [35]. Of course, we cannot exclude the commensurate quantum solid picture only from the present thermodynamic measurements, and new scattering experiments to check possible hexatic modulations in diffraction patterns are highly desirable. In any case, the C2 phase should be the first experimental realization of atomic QLC.

The possible hexatic order in 2D ^4He systems has previously been examined theoretically by several authors [36, 37]. They predict reduced but finite superfluid densities at $T = 0$, the *superhexatic* state. It may help to understand the tiny superfluid fractions observed in the torsional oscillator experiments [12, 13]. In connection with this, let us emphasize an anomalous isotope effect on T_{peak} we found in this experiment. In any previously known quantum solids of He and hydrogen regardless of spatial dimension [15, 23, 28, 31, 32, 38–40], heavier isotopes have “always” slightly lower melting temperatures T_m (or T_{peak}) than lighter ones with the same densities, i.e., $dT_m/dm \leq 0$ (Fig. 3(b)). Here m is atomic or molecular mass. This is because of smaller zero-point motions and hence smaller hardcore repulsion in heavier isotopes [41]. On the other hand, T_{peak} and ΔS are larger by 40% in the ^4He -C2 phase compared to ^3He despite their nearly the same areal densities (see Fig. 3(a)(b)). Clearly an extra degree of freedom other than crystallographic ones stiffens order in the ^4He -C2 phase. Note that the spin entropy change in the ^3He -C2 phase appears only below 100 mK [9]. This singularity is hard to understand unless we assume that the ^4He -C2 specific heat anomaly is associated with the superfluid transition of QLC (supersolid or superhexatic transition) where the superfluidity and crystalline orders vanish simultaneously. The recent topological argument on disclination pairs in 2D QLCs [42] indicates that, by intertwining the two kinds of order, T_m in triangular or hexagonal lattices can substantially be enhanced compared to untwined cases in stripes or square lattices which show successive transitions.

In summary, we determined detailed phase diagrams of the second layer of ^4He and ^3He showing the unambiguous existence of distinct phase (C2 phase) at densities

between the liquid and incommensurate solid phases. It would be the quantum liquid crystal (QLC), a new class of matter, more specifically, the commensurate quantum solid with zero-point defectons or the quantum hexatic phase. In addition, from the anomalously enhanced melting temperature and entropy release in the ^4He -C2 phase, we deduced the possible superfluid QLC state where both spatial and gauge symmetries are spontaneously, partially and simultaneously broken at a temperature below 1.4 K.

We thank Tony Leggett, Hans Lauter, Luciano Reatto and Naoki Kawashima for helpful discussions. This work was financially supported by Grant-in-Aid for Scientific Research on Priority Areas (Grant No. 17071002) from MEXT, Japan and Scientific Research (A) (Grant No. 22244042) from JSPS. S. N. acknowledges support from the Fuuju-kai Fellowship.

* hiroshi@phys.s.u-tokyo.ac.jp

- [1] E. Fradkin, S. A. Kivelson, M. J. Lawler, J. P. Eisenstein, and A. P. Mackenzie, *Ann. Rev. Cond. Matt. Phys.* **1**, 153 (2010).
- [2] E. Frey, D. R. Nelson, and D. S. Fisher, *Phys. Rev. B* **49**, 9723 (1994).
- [3] A. F. Andreev and I. M. Lifshitz, *Sov. Phys. JETP* **29**, 1107 (1969).
- [4] E. Kim and M. H. W. Chan, *Nature* **427**, 225 (2004); D. Y. Kim and M. H. W. Chan, *Phys. Rev. Lett.* **109**, 155301 (2012).
- [5] S. Balibar and F. Caupin, *J. Phys.: Condens. Matter* **20**, 173201 (2008); Y. Vekhov, W. J. Mullin, and R. B. Hallock, *Phys. Rev. Lett.* **113**, 035302 (2014); These articles revealed important roles of superflow along macroscopic or microscopic defects rather than bulk flow in hcp solid ^4He .
- [6] M. Boninsegni and N. V. Prokof'ev, *Rev. Mod. Phys.* **84**, 759 (2012).
- [7] A. B. Vorontsov and J. A. Sauls, *Phys. Rev. Lett.* **98**, 045301 (2007).
- [8] L. V. Levitin, R. G. Bennett1, A. Casey, B. Cowan, J. Saunders, D. Drung, T. Schurig, and J. M. Parpia, *Science* **340**, 841 (2013).
- [9] K. Ishida, M. Morishita, K. Yawata, and H. Fukuyama, *Phys. Rev. Lett.* **79**, 3451 (1997); H. Fukuyama and M. Morishita, *Physica B* **280**, 104 (2000); H. Fukuyama, *J. Phys. Soc. Jpn.* **77**, 111013 (2008).
- [10] Y. Matsumoto, D. Tsuji, S. Murakawa, H. Akisato, H. Kambara, and H. Fukuyama, *J. Low Temp. Phys.* **138**, 271 (2005); S. Murakawa, H. Akisato, Y. Matsumoto, D. Tsuji, K. Mukai, H. Kambara, and H. Fukuyama, *AIP Conf. Proc.* **850**, 311 (2006).
- [11] Y. Fuseya and M. Ogata, *J. Phys. Soc. Jpn.* **78**, 013601 (2009); S. Watanabe and M. Imada, *J. Phys. Soc. Jpn.* **78**, 033603 (2009).
- [12] P. A. Crowell and J. D. Reppy, *Phys. Rev. B* **53**, 2701 (1996).
- [13] Y. Shibayama, H. Fukuyama, and K. Shirahama, *J. Phys.: Conf. Ser.* **150**, 032096 (2009).
- [14] D. Sato, K. Naruse, T. Matsui, and H. Fukuyama, *Phys. Rev. Lett.* **109**, 235306 (2012).
- [15] D. S. Greywall, *Phys. Rev. B* **47**, 309 (1993).
- [16] S. W. Van Sciver and O. E. Vilches, *Phys. Rev. B* **18**, 285 (1978).
- [17] P. Corboz, M. Boninsegni, L. Pollet, and M. Troyer, *Phys. Rev. B* **78**, 245414 (2008).
- [18] F. F. Abraham, J. Q. Broughton, P. W. Leung, and V. Elser, *Europhys. Lett.* **12**, 107 (1990); M. Pierce and E. Manousakis, *Phys. Rev. B* **59**, 3802 (1999); T. Takagi, *J. Phys.: Conf. Ser.* **150**, 032102 (2009).
- [19] Y. Niimi, T. Matsui, H. Kambara, K. Tagami, M. Tsukada, and H. Fukuyama, *Phys. Rev. B* **73**, 085421 (2006); R. J. Birgeneau, P. A. Heiney, and J. P. Pelz, *Physica B+C* **109–110**, 1785 (1982).
- [20] K. J. Strandburg, *Rev. Mod. Phys.* **60**, 161 (1988).
- [21] S. Nakamura, K. Matsui, T. Matsui, and H. Fukuyama, *J. Phys.: Conf. Ser.* **400**, 032061 (2012).
- [22] S. Nakamura, K. Matsui, T. Matsui, and H. Fukuyama, *J. Low Temp. Phys.* **171**, 711 (2013); The T -dependent correction applied to the raw heat-capacity data above 2.2 K in this reference is totally unnecessary in the present experiment.
- [23] S. Nakamura, K. Matsui, T. Matsui, and H. Fukuyama, to appear.
- [24] H. J. Lauter, H. P. Schildberg, H. Godfrin, H. Wiechert, and R. Haensel, *Can. J. Phys.* **65**, 1435 (1987); H. J. Lauter, H. Godfrin, V. L. P. Frank, and P. Leiderer, edited by H. Taub, G. Torzo, H. J. Lauter, and J. S. C. Fain, *Phase Transitions in Surface Films 2* (Plenum Press, New York, 1991) pp. 135–151.
- [25] K. Wierschem and E. Manousakis, *Phys. Rev. B* **83**, 214108 (2011).
- [26] D. M. Ceperley and E. L. Pollock, *Phys. Rev. B* **39**, 2084 (1989).
- [27] D. S. Greywall, *Phys. Rev. B* **41**, 1842 (1990).
- [28] S. W. Van Sciver, *Phys. Rev. B* **18**, 277 (1978); Note that the surface area in this reference has been corrected by -2.5% . See D. S. Greywall and P. A. Busch, *Phys. Rev. Lett.* **65**, 64 (1990).
- [29] Density ratios between the first and second layers are 0.62 ± 0.05 (^4He) and 0.65 ± 0.03 (^3He) which are closer to $2/3 = 0.667$ or $13/19 = 0.684$ rather than $4/7 = 0.571$. Hence our data are not consistent with the previous structural assignment of the $4/7$ phase.
- [30] A. F. Andreev, edited by D. F. Brewer, *Progress in Low Temp. Phys.*, Vol. VIII (North-Holland, Amsterdam, 1982) pp. 67–131.
- [31] M. Bretz, J. G. Dash, D. C. Hickernell, E. O. McLean, and O. E. Vilches, *Phys. Rev. A* **8**, 1589 (1973).
- [32] S. Hering, S. Van Sciver, and O. Vilches, *J. Low Temp. Phys.* **25**, 793 (1976).
- [33] B. I. Halperin and D. R. Nelson, *Phys. Rev. Lett.* **41**, 121 (1978).
- [34] Recently we found that ^3He monolayers adsorbed on graphite preplated with an HD bilayer show a quantum spin-liquid behaviour characteristic to the ^3He -C2 phase at similar densities ($\approx 7 \text{ nm}^{-2}$) though they have a much lower underlayer density by 23%. This is not consistent with the commensurate quantum solid model. The details will be published elsewhere.

- [35] J. Halinen, V. Apaja, K. A. Gernoth, and M. Saarela, J. of Low Temp. Phys. **121**, 531 (2000); E. Krotscheck and T. Lichtenegger, *ibid.* **178**, 61 (2015).
- [36] K. Mullen, H. T. C. Stoof, M. Wallin, and S. M. Girvin, Phys. Rev. Lett. **72**, 4013 (1994).
- [37] V. Apaja and M. Saarela, Europhys. Lett. **84**, 40003 (2008); In this calculation for a pure 2D ^4He system the hexatic correlation appears at densities above 6.5 nm^{-2} and the solid phase becomes stable above 7.0 nm^{-2} , while, in our experiment, the C2 correlation appears between 6.9 and 8.4 nm^{-2} and is maximized at 7.7 nm^{-2} .
- [38] H. Wiechert, Physica B: Condensed Matter **169**, 144 (1991).
- [39] E. R. Grilly and R. L. Mills, Ann. Phys. **8**, 1 (1959).
- [40] D. H. Liebenberg, R. L. Mills, and J. C. Bronson, Phys. Rev. B **18**, 4526 (1978).
- [41] D. S. Hirashima, T. Momoi, and T. Takagi, J. Phys. Soc. Jpn. **72**, 1446 (2003).
- [42] S. Gopalakrishnan, J. C. Y. Teo, and T. L. Hughes, Phys. Rev. Lett. **111**, 025304 (2013).